Projectile-charge dependence of the differential cross section for the ionization of argon atoms at 1 keV

G. Purohit[1,2] and D. Kato[1,3,4]

[1]*National Institute for Fusion Science, National Institutes of Natural Sciences 322-6 Oroshi-cho, Toki Gifu, 509-5292, Japan*
[2]*Department of Physics, Sir Padampat Singhania University, Bhatewar, Udaipur-313601, India*
[3]*Department of Fusion Science, SOKENDAI, 322-6 Oroshi-cho, Toki Gifu, 509-5292, Japan*
[4]*Department of Advanced Energy Engineering, Kyushu University, Kasuga Fukuoka, 816-8580, Japan*

The single ionization triple differential cross sections (TDCS) of the Ar $(3p)$ atoms are reported for the positron and electron impact at 1 keV. The calculated cross sections have been obtained using distorted wave Born approximation (DWBA) approach for the average ejected electron energies 13 and 26 eV at different momentum transfer conditions. The present attempt is helpful to probe the information on the TDCS trends for the particle-matter and antiparticle-matter interactions and to analyze the recent measurements [Phy. Rev. A **95**, 062703 (2017)]. The binary electron emission is enhanced while the recoil emission is decreased for the positron impact relative to the electron impact in the DWBA calculation results. Systematic shift of peaks, shifting away from the momentum transfer direction for positron impact and shifting towards each other for electron impact, is observed with increasing momentum transfer.

I. INTRODUCTION

Ionization of targets such as atoms, ions, and molecules by charged projectiles such as electrons has been studied for a long time and has various applications; a few are diagnostics of fusion plasmas, modeling of physics and chemistry related to the atmosphere, understanding the effect of ionizing radiation on biological tissues, etc. Detailed information about this kind of collision process is obtained from the triple differential cross sections (TDCS) obtained through a coincidence study, which has been of interest since the pioneering work of Ehrhardt group [1]. A coincidence study of TDCS has been of particular interest since it provides full information about the collision dynamics and momentum vectors of all free particles involved in the ionization are determined. Significant progress has been made to investigate the electron impact single ionization of atomic hydrogen and atomic helium targets, and reliable theoretical results, based on perturbative as well as nonperturbative formalism, of TDCS have been obtained which give very good agreement with the experimental results [2–6]. Efforts have also been made to calculate TDCS for the light alkali and alkaline-earth metals, and reasonable agreement with the measurements has been obtained [7,8]. Compared to the above mentioned targets, the treatment of heavier complex targets such as noble gases Ne-Xe is difficult, and the progress made to date has been slower. Recently the B-Spline R-Matrix (BSR) approach has been found very successful in describing the ionization of He atoms [9,10], and it has also been applied to heavier noble gas targets such as Ar [11,12] in the low and intermediate energy ranges. Recently few more efforts, experimental as well as theoretical, have been made to describe the ionization from Ar $(3p)$ atoms in asymmetric kinematics at low to intermediate energy ranges [13–15]. Thus, so far a good understanding of the electron impact ionization process has been obtained.

Some recent work using antimatter-antiparticle projectile has drawn the attention of researchers in the field [16,17]. Such kinds of studies are helpful to obtain information about the similar or different features of the particle-matter and antiparticle-matter interactions. There has been demand for differential cross section studies with positrons for a long time, which has mainly remained confined to single differential and double differential investigations [18,19]. The projectile target interaction is better probed by the differential ionization data; they give information about energy and momentum transfer, and in particular the positron impact studies are desirable to probe the role of projectile charge or mass on the collision dynamics in comparison to the electrons having similar kinematics conditions and also has important applications in characterization of materials, PET imaging in medicines, etc. [20]. Very few experimental and theoretical TDCS data are available for the positron impact ionization. Positron impact TDCS results have been reported for the ionization of He atoms and H_2 molecules [21]. Measurement for the positron impact ionization of Ar $(3p)$ has been reported in the intermediate energy range [22], following which TDCS has been calculated in the distorted wave Born approximation (DWBA) formalism [23]. A coincidence study of electron and positron impact ionization of Ar $(3p)$ has been reported at the projectile energy 1 keV [24] describing the comparison between the calculated TDCS results with the measurements [25]. Very recently triple differential measurements of single ionization of argon atoms by 1 keV positron and electron impact have been reported by Gavin *et al.* [26]. In this study, the triple differential cross section information has been generated in terms of the projectile energy loss and scattering angles for the interactions between 1 keV positrons and electrons with Ar atoms.

Following the recent positron and electron impact differential measurements on argon atoms [26], we report the theoretical results of TDCS for all the kinematic options for which the TDCS measurements have been reported. Our present attempt is useful to analyze the recent measurements for which no other theoretical results, to the best of our knowledge, are available to compare. We report the TDCS

results calculated in the distorted wave Born approximation (DWBA) formalism, which should be of significance and sufficient at the high impact energy of 1 keV and good enough to give the first estimates of comparison with the measurements. The present attempt is useful to understand the salient features observed in the TDCS of argon atoms due to projectile charge. The atomic units ($\hbar = e = m_e = 1$) have been used in the present paper. The brief description of theoretical formalism is presented in the next section.

A. Theory

The electron-positron impact single ionization of Ar atoms is defined as

$$e^-/e^+ + \text{Ar} \rightarrow \text{Ar}^+ + e^-/e^+ + e^-. \qquad (1)$$
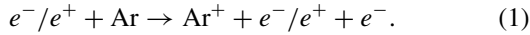
In this reaction a projectile (electron or positron) with energy E_0 and momentum k_0 collides with the target atoms and produces a scattered electron or positron and an ejected electron with energies E_1, E_2 and momenta k_1, k_2 respectively in the outgoing channel, which are observed in coincidence. The triple differential cross section (TDCS) for the electron-positron impact single ionization [Eq. (1)], which is the probability of single ionization, is expressed in atomic units as

$$\frac{d^3\sigma}{d\Omega_1\, d\Omega_2\, dE_1} = (2\pi)^4 \frac{k_1 k_2}{k_0} \sum_{av} |T(k_1, k_2, k_0)|^2 \qquad (2)$$

with

$$T(k_1, k_2, k_0) = \langle k_1 k_2 | T | \psi_{nl} k_0 \rangle.$$

The T matrix in Eq. (2) includes interaction between the projectile and target electrons and the nucleus.

B. Electron impact

TDCS [Eq. (2)] for the ionization from the nl orbital is written as

$$\frac{d^3\sigma}{d\Omega_1\, d\Omega_2\, dE_1}$$
$$= (2\pi)^4 \frac{k_1 k_2}{k_0} \sum_{m=-l}^{l} (|f_{nlm}|^2 + |g_{nlm}|^2 - \text{Re}(f_{nlm}^* g_{nlm}))$$
$$(2)$$

where

$$f_{nlm} = \langle X_1^{(-)}(k_1, r_1)\, X_2^{(-)}(k_2, r_2)\, |v_3|\, X_0^{(+)}(k_0, r_1)\, \psi_{nl}(r_2) \rangle, \qquad (3)$$

$$g_{nlm} = \langle X_1^{(-)}(k_1, r_2)\, X_2^{(-)}(k_2, r_1)\, |v_3|\, X_0^{(+)}(k_0, r_1)\, \psi_{nl}(r_2) \rangle; \qquad (4)$$

here $v_3 = \frac{1}{|r_1 - r_2|}$ is the interaction potential between the incident and target electrons responsible for the ionization, The distorted wavefunction for the incident electron is represented by $X_0^{(+)}$. $X_1^{(-)}$ and $X_2^{(-)}$ represent the distorted wavefunctions for the two outgoing electrons, and each is orthogonalized with

respect to ψ_{nl}. Equations (3) and (4) are direct and exchange amplitudes for ionization from the (n,l) shell of the target atom where ψ_{nl} is the corresponding target orbital from which the ionization is taking place, and n and l are the principal and orbital quantum numbers, respectively. The potentials are obtained from the Hartree-Fock functions of Clementi and Roetti [27] and localized version of exchange potential is employed [28,29], which simplifies the static-exchange calculations.

C. Positron impact

For the positron impact ionization there is no exchange amplitude g_{nlm}, and the following choices have been made: the distorted waves for the incident ($X_0^{(+)}$) and scattered ($X_1^{(-)}$) positrons are generated in the static potential of the Ar atom, and the distorted waves for the ejected electron ($X_2^{(-)}$) are generated in the static exchange potential of the Ar$^+$ ion.

We have also included target polarization potential for the calculation of distorted waves in the case of electron-positron impact ionization, but the results of TDCS obtained are nearly similar as the TDCS without inclusion of polarization potential so not displayed in all the figure frames [see the dotted curve in Fig. 1(d)]. The results and discussion are summarized in the next section.

II. RESULTS AND DISCUSSION

The TDCS results for the positron and electron impact ionization of Ar ($3p$) at 1 keV projectile energy are presented in Figs. 1–6. The present DWBA results are compared with the recent measurements [26]. The solid curve is the DWBA calculation for the positron impact, and the dashed curve represents DWBA results for the electron impact. Solid circles (black) are the experimental data for electron impact, and the solid circles (red) are the experimental data for positron impact. The experimental data have been normalized to the positron impact DWBA cross sections to give the best fit for visualization while retaining the relative normalization between the positron and electron measurements as well as the relative normalization with scattering angles. The TDCS results for the average ejected electron energy 26 eV and scattering angles 1.2°, 2.1°, and 2.9° are presented in Fig. 1. The left column [Figs. 1(a)–1(c)] displays the TDCS results for the positron impact, and the right column [Figs. 1(d)–1(f)] displays the TDCS results for the electron impact. Two separate regions termed binary collision and recoil collision are observed in the measurements as well as in the present calculations for both the positron and electron impact. The present DWBA results disagree with the measurements in terms of the shape of cross sections and relative magnitude of cross sections for positron and electron impact ionization. The recoil peak height in the measurement is nearly comparable to the binary peak height at scattering angle 1.2° [Fig. 1(a)], which is not observed in the theoretical results. The binary and recoil peak splitting is not observed as predicted by the visual fits to the experimental data [26].

TDCS results for the average ejected electron energy 13 eV and scattering angles 1.2°, 2.1°, and 2.9° are presented in Fig. 4. The symbols and legends are same as defined earlier.
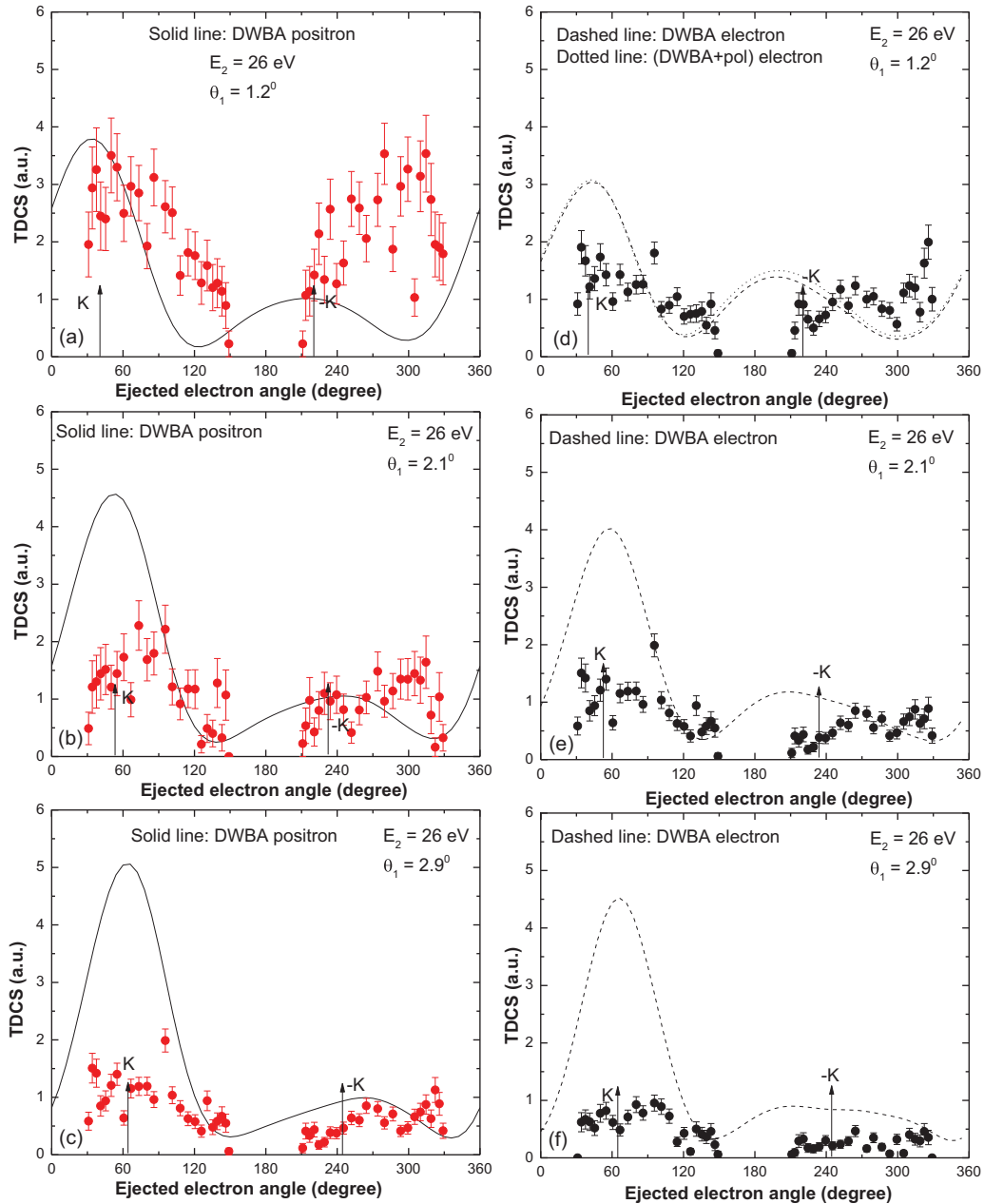
FIG. 1. TDCS plotted as a function of ejected electron angle for the ionization of Ar ($3p$) at ejected electron energy 26 eV. Panels (a)–(c) for positron impact and frames (d)–(f) electron impact ionization. Solid curve: DWBA calculation for positron impact; dashed curve: DWBA calculation for electron impact; dotted curve: DWBA + polarization potential calculation; red circles: experimental data [26] for positron impact; black circles: experimental data [26] for electron impact. Scattering angles are displayed in each frame, and experimental data have been normalized to the solid curve and dashed curve in the binary peak region for best visual fit while retaining the relative normalization between the positron and electron data as well as the relative normalization with scattering angles.

The DWBA cross sections disagree with the measurement for this case also in terms of shape and magnitude. The fit to the measurements [26] (Fig. 7 in Ref. [26]) predict splitting of the recoil peaks for the positron impact and splitting of binary peaks as well as recoil peaks for the electron impact; however, the present DWBA results do not show the splitting of the peaks for these scattering angles.

We observe larger binary peaks for positron impact compared to electron impact and larger recoil peaks for electron impact compared to positron impact [Figs. 2(a)–2(c), and 5(a)–5(c)] at both the ejected electron energies 26 and 13 eV; however, the measurements show both the binary and recoil peak intensities higher for positron impact in comparison to electron impact. Splitting of the binary and recoil peaks is observed in the present DWBA calculations for the higher scattering angles [Figs. 3(b), and 6(b)]; however, the fits to the measurements [26] also predict the splitting for smaller scattering angles, which needs further theoretical efforts to
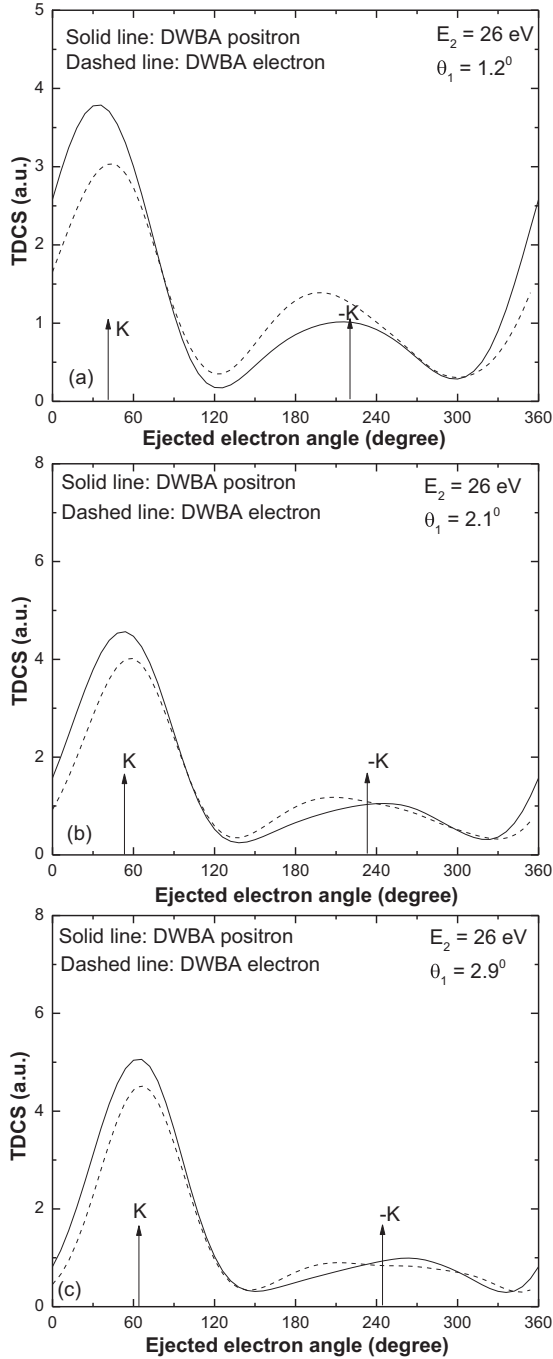
FIG. 2. Positron and electron impact TDCS for the Ar $(3p)$ plotted as a function of ejected electron angle for the ionization of Ar $(3p)$ at ejected electron energy 26 eV at scattering angles (a) 1.2°, (b) 2.1°, and (c) 2.9°. Solid curve: DWBA calculation for positron impact; dashed curve: DWBA calculation for electron impact.

FIG. 3. TDCS plotted as a function of ejected electron angle for the ionization of Ar $(3p)$ at ejected electron energy 26 eV at scattering angles (a) 5° and (b) 10°. The legends are the same as Fig. 2.

verify. The splitting of binary peak is more pronounced for the positron impact ionization at ejected electron energy 13 eV [Fig. 6(b)]. We have also included target polarization in the present DWBA calculations, but it is observed that nearly similar TDCS is obtained without inclusion of target polarization [see dotted and dashed curves in Figs. 1(d) and 4(d)], so we have not plotted the curves with target polarization in all the frames. We have also included postcollision interaction
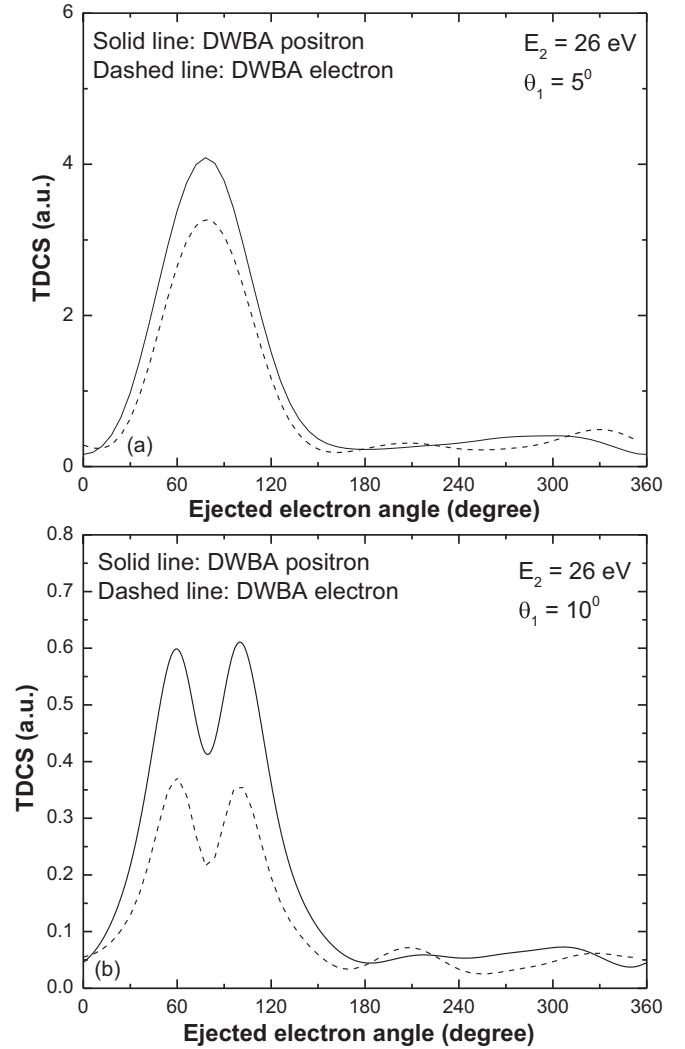
using the Ward-Macek factor [30] and observed that PCI is not significant to describe TDCS in the present kinematics (so curves are not shown here), as also observed by the recent theoretical work for the nearly similar kinematics [24].

The recoil-to-binary peak ratio obtained in DWBA calculations for both the average ejected electron energies (13 and 26 eV) for the positron and electron impact ionization are summarized in Table I for different values of scattering angles (momentum transfer). The obtained values of the recoil-to-binary peak ratio suggest that at both ejected electron energies the binary emission of the electron is enhanced for the positron impact ionization, and the recoil emission of the electron, which is due to interaction of ejected electron with target nucleus, is decreased for the positron impact ionization. The observed ratio also suggest that the recoil peak is more pronounced for the lower ejected electron energy (i.e., 13 eV) for positron as well as electron impact. However, it is observed by measurements [26] that both the binary and recoil emission of electrons is enhanced for the positron impact in comparison to the electron impact, which needs further
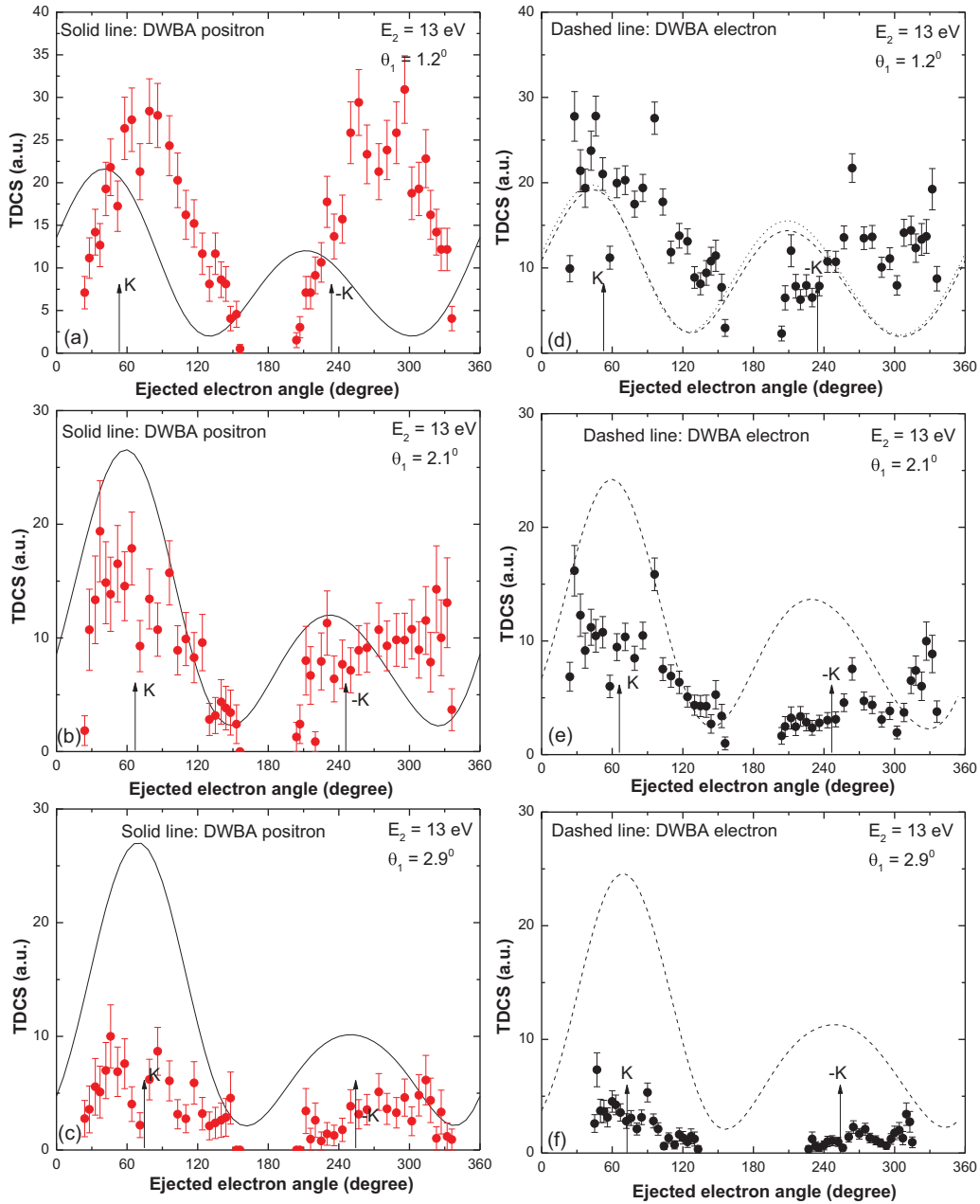
FIG. 4. TDCS plotted as a function of ejected electron angle for the ionization of Ar $(3p)$ at ejected electron energy 13 eV. Frames (a)–(c) for positron impact and frames (d)–(f) electron impact ionization. The legends are the same as Fig. 1, the scattering angles are displayed in each frame, and experimental data have been normalized to solid curve and dashed curve in the binary peak region for best visual fit while retaining the relative normalization between the positron and electron data as well as the relative normalization with scattering angles.

theoretical investigations. We observe that the binary and recoil peaks are obtained in the direction of momentum transfer and its opposite (arrows shown in each figure frames) in the DWBA results for positron impact ionization at smaller scattering angle and higher ejected electron energy [Fig. 1(a)]; however, as momentum transfer increases, the peaks shift towards higher ejected electron angles (more shift for recoil lobe). At the lower ejected electron energy (i.e., 13 eV), the binary as well as recoil peaks are shifted towards lower ejected electron angles [Fig. 4(a)] and as momentum transfer increases, the peaks shift towards higher ejected electron angles. In the case of electron

impact both the binary and recoil peaks shifts towards each other as the momentum transfer increases.

III. CONCLUSIONS

We have reported the positron and electron impact ionization differential cross section results for the Ar $(3p)$ atoms at average electron energies 26 and 13 eV for the different momentum transfer conditions (scattering angles). Present attempt helps to probe the antiparticle-matter and particle-matter interactions, and it is observed that the DBWA is able to produce the differences in the trends of TDCS, which are pro-
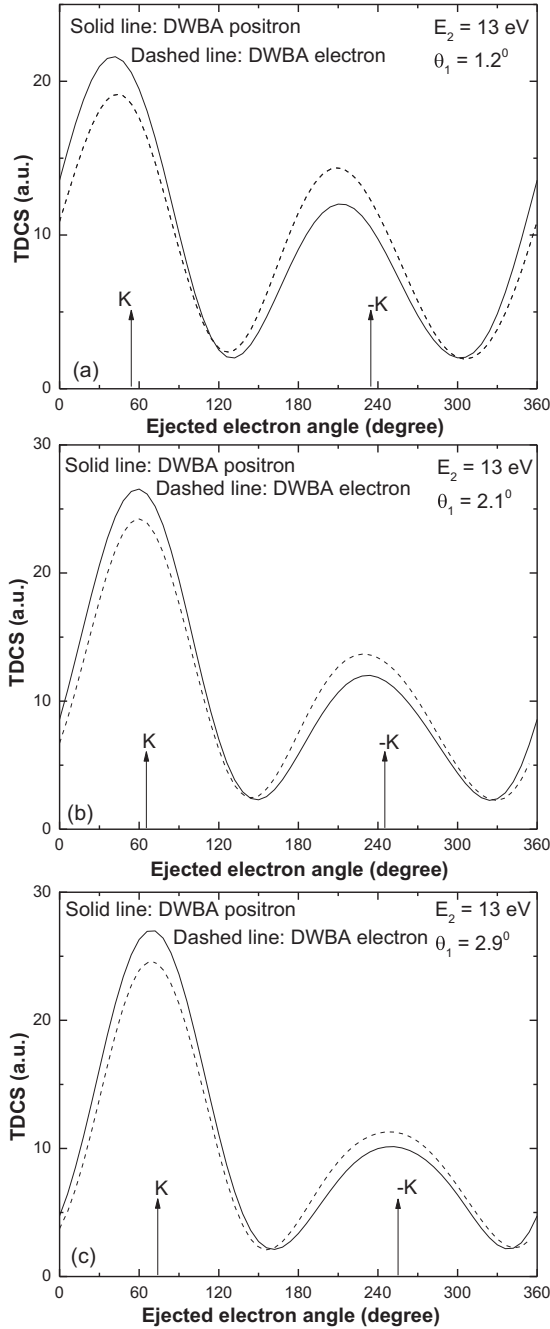
FIG. 5. Positron and electron impact TDCS for the Ar $(3p)$ plotted as a function of ejected electron angle for the ionization of Ar $(3p)$ at ejected electron energy 13 eV at scattering angles (a) 1.2°, (b) 2.1°, and (c) 2.9°. Solid curve: DWBA calculation for positron impact; dashed curve: DWBA calculation for electron impact.

FIG. 6. TDCS plotted as a function of ejected electron angle for the ionization of Ar $(3p)$ at ejected electron energy 13 eV at scattering angles (a) 5° and (b) 10°. The legends are the same as Fig. 5.

scattering angle. There are large discrepancies in terms of peak positions and relative magnitudes. The binary electron emission is increased for positron impact and the recoil emission is decreased; however, in the case of measurements both the binary and recoil emission increases for positron

jectile charge dependent. DWBA results have been compared with the recent measurements [26]. The measurements indicate that the positron impact TDCS are larger than the electron impact TDCS for all the cases. The measurements also exhibit the decrease of relative intensities of both the binary and recoil peaks as momentum transfer is increased. The present DWBA results do not show the decrement of the magnitude of binary peak; however, the magnitude of recoil peak decreases but not as observed in the experiments with increase of
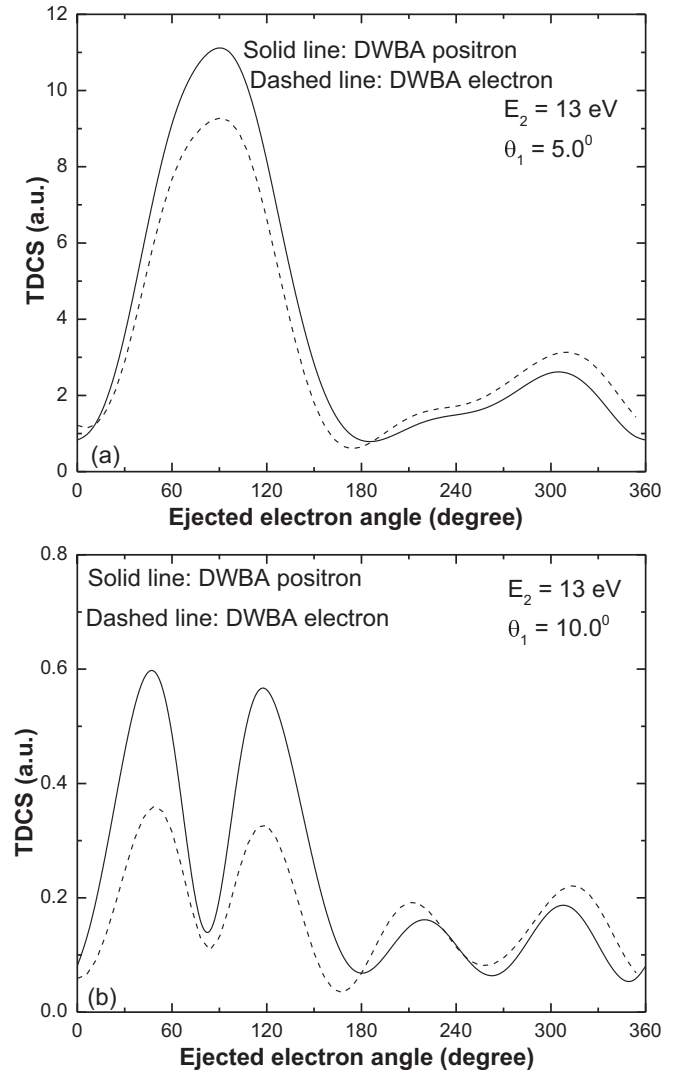
TABLE I. TDCS recoil-to-binary peak ratio (r/b) observed in the DWBA calculations for the Ar $(3p)$ ionization at 1 keV projectile energy.

Average ejected electron energy	Projectile	Recoil-to-binary peak ratio (r/b)		
		Scattering angle 1.2°	Scattering angle 2.1°	Scattering angle 2.9°
13 eV	Positron impact	0.55	0.45	0.37
	Electron impact	0.74	0.56	0.46
26 eV	Positron impact	0.27	0.23	0.19
	Electron impact	0.46	0.29	0.20

impact, which may be of interest for further investigation. Systematic shift of peaks, shifting away from the momentum transfer direction for positron impact and shifting towards each other for electron impact, is observed with increasing momentum transfer. The postcollision interaction and target polarization has not been found significant, further theoretical efforts with accurate treatment for electron exchange may be important to understand the disagreement with the experiments.

[1] H. Ehrhardt, K. H. Hesselbacher, K. Jung, and K. Willmann, J. Phys. B **5**, 1559 (1972).

[2] D. H. Madison, Phys. Rev. Lett. **53**, 42 (1984).

[3] K. Bartschat and O. Vorov, Phys. Rev. A **72**, 022728 (2005).

[4] T. N. Rescigno, M. Baertschy, W. A. Isaacs, and C. W. McCurdy, Science **286**, 2474 (1999).

[5] I. Bray, D. V. Fursa, A. S. Kheifets, and A. T. Stelbovics, J. Phys. B **35**, R117 (2002).

[6] J. Colgan, O. Al-Hagan, D. H. Madison, A. J. Murray, and M. S. Pindzola, J. Phys. B **42**, 171001 (2009).

[7] G. Purohit, V. Patidar, and K. K. Sud, Phys. Lett. A **374**, 2654 (2010).

[8] G. Purohit, Prithvi Singh, Vinod Patidar, Y. Azuma, and K. K. Sud, Phys. Rev. A **85**, 022714 (2012).

[9] O. Zatsarinny and K. Bartschat, Phys. Rev. Lett. **107**, 023203 (2011).

[10] O. Zatsarinny and K. Bartschat, Phys. Rev. A **85**, 062709 (2012).

[11] O. Zatsarinny and K. Bartschat, Phys. Rev. A **85**, 032708 (2012).

[12] X. Ren, T. Pflüger, J. Ullrich, O. Zatsarinny, K. Bartschat, D. H. Madison, A. Dorn, and J. Ullrich, Phys. Rev. A **85**, 032702 (2012).

[13] S. Amami, M. Ulu, Z. N. Ozer, M. Yavuz, S. Kazgoz, M. Dogan, O. Zatsarinny, K. Bartschat, and D. Madison, Phys. Rev. A **90**, 012704 (2014).

[14] X. Ren, S. Amami, O. Zatsarinny, T. Pfluger, M. Weyland, A. Dorn, D. Madison, and K. Bartschat, Phy. Rev. A **93**, 062704 (2016).

[15] S. Amami, Z. N Ozer, M. Dogan, M. Yavuz, O. Varol, and D. Madison, J. Phys. B: At. Mol. Opt. Phys. **49**, 185202 (2016).

[16] G. Laricchia, S. Armitage, A. Kover, and D. J. Murtagh, Adv. At. Mol. Opt. Phys. **56**, 1 (2008).

[17] M. McGovern, D. Assafrao, J. R. Mohallem, C. T. Whelan, and H. R. J. Walters, Phys. Rev. A **79**, 042707 (2009).

[18] A. Kover, R. M. Finch, M. Charlton, and G. Laricchia, J. Phys. B **30**, L507 (1997).

[19] A. C. F. Santos, A. Hasan, and R. D. DuBois, Phys. Rev. A **69**, 032706 (2004).

[20] G. Laricchia *et al.*, Radiat. Phys. Chem. **68**, 21 (2003).

[21] R. I. Campeanu, Nucl. Instr. Meth. B **267**, 239 (2009)

[22] O. G. de Lucio, S. Otranto, R. E. Olson, and R. D. DuBois, Phys. Rev. Lett. **104**, 163201 (2010).

[23] G. Purohit, V. Patidar, and K. K. Sud, Nucl. Inst. Meth. Phy. Res. B **269**, 745 (2011).

[24] R. I. Campeau, J. H. R. Walters, and C. T. Whelan, Eur. Phys. J. D **69**, 235 (2015).

[25] R. D. DuBois, J. Gavin, and O. G. de Lucio, J. Phys. Conf. Ser. **488**, 072004 (2014).

[26] J. Gavin, O. G. de Lucio, and R. D. DuBois, Phy. Rev. A **95**, 062703 (2017).

[27] E. Clementi and C. Roetti, At. Data Nucl. Data Tab. **14**, 177 (1974).

[28] J. B. Furness and I. E. McCarthy, J. Phys. B **6**, 2280 (1973).

[29] M. E. Riley and D. G. Truhlar, J. Chem. Phys. **63**, 2182 (1975).

[30] S. J. Ward and J. H. Macek, Phys. Rev. A **49**, 1049 (1994).